

Sequentially Linear Analysis of Structures with Stochastic Material Properties

George Stefanou, Manolis Georgioudakis, and Manolis Papadrakakis

Abstract This paper investigates the influence of uncertain spatially varying material properties on the fracture behavior of structures with softening materials. Structural failure is modeled using the sequentially linear analysis (SLA) proposed by Rots (Sequentially linear continuum model for concrete fracture. In: de Borst R, Mazars J, Pijaudier-Cabot G, van Mier J (eds) Fracture mechanics of concrete structures. Balkema, Lisse, 2001, pp 831–839), which replaces the incremental nonlinear finite element analysis by a series of scaled linear analyses and the nonlinear stress-strain law by a saw-tooth curve. In this work, SLA is implemented in the framework of a stochastic setting. The proposed approach constitutes an efficient procedure avoiding the convergence problems encountered in regular nonlinear FE analysis. The effect of uncertain material properties (Young's modulus, tensile strength, fracture energy) on the variability of the load-displacement curves and crack paths is examined. The uncertain properties are described by homogeneous stochastic fields using the spectral representation method in conjunction with translation field theory. The response variability is computed by means of direct Monte Carlo simulation. The influence of the variation of each random parameter as well as of the coefficient of variation and correlation length of the stochastic fields is quantified in a numerical

G. Stefanou (✉)

Institute of Structural Analysis & Antiseismic Research, National Technical University of Athens, 9 Iroon Polytechniou, Zografou Campus, Athens 15780, Greece

Institute of Structural Analysis & Dynamics of Structures, Aristotle University of Thessaloniki, 54124 Thessaloniki, Greece

e-mail: stegesa@mail.ntua.gr

M. Georgioudakis • M. Papadrakakis

School of Civil Engineering, Institute of Structural Analysis & Antiseismic Research, National Technical University of Athens, Zografou Campus, 15780 Athens, Greece

e-mail: geoem@mail.ntua.gr; mpapadra@central.ntua.gr

example. It is shown that the load-displacement curves, the crack paths and the failure probability are affected by the statistical characteristics of the stochastic fields.

Keywords Softening materials • Sequentially linear analysis • Stochastic field • Response variability • Monte Carlo simulation

1 Introduction

Several numerical techniques have been recently developed to model the failure of structures in the framework of the finite element method (FEM). For structures made of softening materials, a realistic representation of the softening behavior requires the accurate description of stiffness degeneration due to damage. This description can be achieved in a unified manner using damage mechanics approaches that have been proven advantageous for modeling failure phenomena due to their numerical efficiency. The damage mechanics approach permits the incorporation of the description of damage into the constitutive equations, as well as the combination with different more specific simulation methods, such as the embedded finite element method (Oliver 1996; Oliver et al. 2012), extended finite element method (Moës et al. 1999; Mariani and Perego 2003) and non-local theories (Jirásek 1998).

It is also known in failure mechanics that material softening is often responsible for unstable structural behavior (Bažant and Cedolin 2010). This instability can lead to secondary equilibrium states or bifurcation of the equilibrium path, which require more elaborate incremental/iterative solution schemes (De Borst et al. 2012). As a consequence, the robustness of the numerical procedure used for solving the nonlinear problem is strongly affected. In order to overcome these problems, an alternative method, called sequentially linear analysis (SLA), has been introduced by Rots (2001). This method replaces the incremental nonlinear FE analysis by a series of scaled linear analyses and the nonlinear stress-strain law by a saw-tooth curve. The advantage of this replacement is that the secant linear (saw-tooth) stiffness is always positive and the analysis does always converge. The method is generally applicable for materials with nonlinear softening behavior, but it is particularly beneficial when brittle fracture causes convergence issues. In this paper, SLA is implemented in the framework of a stochastic setting. The proposed approach constitutes an efficient procedure for investigating the influence of uncertain spatially varying material properties on the fracture behavior of structures with softening materials (Georgioudakis et al. 2014).

A benchmark structure (double-edge notched specimen) is analyzed and comparisons with nonlinear analysis results are provided. The effect of uncertain variables such as Young's modulus, tensile strength and fracture energy on the variability of the load-displacement curves and crack paths is examined. The uncertain properties are described by homogeneous stochastic fields using the spectral representation method in conjunction with the translation field theory (Shinozuka and Deodatis

1996; Grigoriu 1998). The response variability is computed by means of direct Monte Carlo simulation (MCS). The influence of the variation of each random parameter as well as of the coefficient of variation and correlation length of the stochastic fields is quantified. It is shown that the response statistics and the failure probability of the structure are affected by the statistical characteristics of the stochastic fields.

2 Sequentially Linear Analysis (SLA)

When analyzing material failure with standard nonlinear FE analysis, problems are often encountered such as bifurcation and divergence of the solution. In particular, cases subjected to tension softening tend to encourage the emergence of multiple equilibrium paths. In order to overcome these problems, the SLA has been developed to address specifically the difficulty of modeling snap-back behavior (Rots 2001), typical in full-scale concrete and masonry structures (DeJong et al. 2009). While generally applicable for materials with nonlinear softening branches, it is particularly beneficial when brittle fracture causes convergence issues.

In SLA, a series of linear analyses are used to model the nonlinear behavior of the structure while the modeling proceeds by directly capturing brittle events, rather than trying to iterate around these critical points in a Newton-Raphson scheme. Hence extensive iterations within the load or displacement increment can be avoided. Furthermore, in this approach, a tensile softening curve of negative slope is replaced by a saw-tooth curve which maintains a positive tangent stiffness (see Fig. 1). The incremental/iterative Newton-Raphson method is no longer required since a series of linear analyses are performed, each with a reduced positive stiffness,

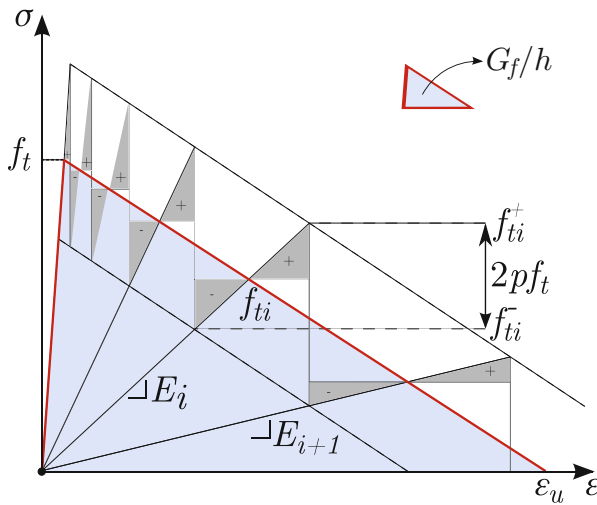


Fig. 1 Stress-strain curve for linear softening and saw-tooth model definitions

Algorithm 1 Sequentially linear analysis

```

1: repeat
2:    $\mathbf{K}_N \mathbf{d}_N = \mathbf{P} \rightarrow \sigma_{i_{pr}}$ 
3:   for  $element = 1, \dots, TotalElements$  do
4:     for  $GaussPoint = 1, \dots, TotalGPperElement$  do
5:       Calculate  $\frac{f_{i_i}^+}{\sigma_{i_{pr}}}$  and find  $\lambda_{crN} = \max\{\frac{f_{i_i}^+}{\sigma_{i_{pr}}}\}$ 
6:     end for
7:   end for
8:   Scale displacements and stress resultants  $(\sigma_N, \mathbf{d}_N)$  by factor  $\lambda_{crN}$ 
9:   for  $element = 1, \dots, TotalElements$  do
10:    for  $GaussPoint = 1, \dots, TotalGPperElement$  do
11:      Find new  $f_{i_i+1}^+, E_{i+1}$  according to Section 2.2
12:    end for
13:  end for
14:  Update structure stiffness matrix  $\mathbf{K}_{N+1} \leftarrow \mathbf{K}_N$ 
15: until damage has spread sufficiently into the structure

```

until the global equilibrium position is achieved. It has been shown that this *event-by-event* strategy is robust and reliable (Rots and Invernizzi 2004), and circumvents bifurcation problems, in contrast to standard nonlinear FE analysis. A more detailed description of the SLA procedure is provided in the following subsections.

2.1 General Procedure

The structure is discretized in the framework of FEM, using standard continuum elements and all material properties (Young's modulus E , Poisson's ratio ν , initial strength f_i , as well as fracture energy G_f) are assigned to them. Subsequently, the following steps are carried out sequentially without the need of changing the initial mesh (see Algorithm 1).

Initially, a linear elastic FE analysis is performed (\mathbf{K}_N : stiffness matrix of the structure and \mathbf{d}_N : vector of unknown displacements in analysis step N) with a reference proportional load \mathbf{P} (line 2). After the calculation of maximum principal tensile stresses ($\sigma_{i_{pr}}$) through the linear elastic analysis, a loop over all integration points for all elements is performed in order to find the *critical element* for which its current strength $f_{i_i}^+$ divided by the maximum principal tensile stress is the highest in the whole structure (lines 3–7). Subsequently (line 8), the reference load \mathbf{P} (along with the corresponding displacements and stress resultants) is scaled proportionally by the critical load multiplier λ_{crN} belonging to the critical integration point. Finally (lines 9–13), the damage in the critical integration point is increased by reducing the stiffness E and strength f_i according to the saw-tooth tensile-based constitutive relation (see Sect. 2.2). The aforementioned procedure is repeated sequentially, until the damage has spread sufficiently into the structure.

In this way, the nonlinear response is extracted by linking consecutively the results of each cycle. The smoothness of $P - \delta$ curves depends on the smoothness

(number N_t of teeth) of the saw-tooth model (see Sect. 2.2). The SLA procedure allows only one integration point to change its status from elastic to softening at each time, while in nonlinear FE analysis, the use of load increments implies that multiple integration points may crack simultaneously and the local stiffnesses at these points switch from positive to negative, following the softening constitutive laws for quasi-brittle materials.

2.2 Saw-Tooth Model

Several saw-tooth approximations could be specified by adjusting the stiffness, maximum strain and strength of each consecutive saw-tooth. However, the approximation must yield results that are mesh independent. Rots and Invernizzi (2004) investigated several saw-tooth approximations and concluded that any approximation must conserve the dissipated energy, i.e. the area under the softening curve, G_f/h (see Fig. 1).

In this work, the generalized tooth size approach (MODEL C) (Rots et al. 2008) is adopted, which does not require special techniques to handle mesh-size objectivity in order to obtain objective results with respect to the mesh as well as to overcome the lack of consistency. The way in which the stiffness and strength of the critical elements are progressively reduced at each “event”, is shown schematically in Fig. 1 where the softening curve of negative slope in the constitutive stress-strain relation is replaced by a discretized, saw-tooth diagram of positive slopes which provides the correct energy dissipation. The linear tensile softening stress-strain curve is defined by the Young’s modulus E , the tensile strength f_t and the area under the saw-tooth diagram. This area (see Fig. 1) is always equal to the fracture energy G_f , which is considered here as a material property, divided by the crack bandwidth h , which is associated with the size, orientation and integration scheme of the finite element.

In case of linear softening, ultimate strain ϵ_u is given by:

$$\epsilon_u = \frac{2G_f}{f_t h} \quad (1)$$

Both Young’s modulus E and strength f_t can be reduced at the same time in the sequentially linear strategy by a factor a , according to:

$$E_i = \frac{E_{i-1}}{a}, \quad \text{for } i = 1, 2, \dots, N \quad (2)$$

where i and $i - 1$ denote the current and previous step, respectively, in the saw-tooth diagram. To find the rule of reducing Young’s modulus E as well as strength f_t , by ratio a_i in step i according to Fig. 1, we have:

$$f_{ti}^- = f_{ti}^+ - 2pf_t \quad (3)$$

$$E_{i+1} = \frac{f_{ti}^-}{\epsilon_i} \quad (4)$$

$$a_{i+1} = \frac{E_i}{f_{ti}^-} \epsilon_i = \frac{f_{ti}^+}{f_{ti}^-} = \frac{f_{ti}^+}{f_{ti}^+ - 2pf_t} \quad (5)$$

Thus, for the case of linear softening (Fig. 1) the value of f_{ti}^+ can be easily defined as:

$$f_{ti}^+ = \epsilon_u^+ E_i \frac{D}{E_i + D} \quad (6)$$

where,

$$\epsilon_u^+ = \epsilon_u + p \frac{f_t}{D} \quad (7)$$

and D is the tangent to the tensile stress-strain softening curve. The number N_t of teeth is automatically evaluated, depending on the user specified parameter p . For smaller values of p , a higher N_t is needed to cover the softening branch, leading to more exact results. The procedure ends, regarding the corresponding Gauss point, when the difference between the sum of *positive* triangles above the real curve and the sum of *negative* triangles below the real curve vanishes, as shown in Fig. 1.

3 Representation of Uncertain Material Properties

3.1 Non-Gaussian Translation Fields

As the Gaussian assumption for variables bounded by physical constraints (e.g. material properties that should be strictly positive) may lead to a non-zero probability of violation of these constraints, the simulation of non-Gaussian stochastic processes and fields has received considerable attention in the field of computational stochastic mechanics.

Since all the joint multi-dimensional density functions are needed to fully characterize a non-Gaussian stochastic field, a number of studies have been focused on producing a more realistic (approximate) definition of a non-Gaussian sample function from a simple transformation of some underlying Gaussian field with known second-order statistics. Thus, if $g(\mathbf{x})$ is a homogeneous zero-mean Gaussian field with unit variance and spectral density function (SDF) $S_{gg}(\boldsymbol{\kappa})$, or equivalently autocorrelation function $R_{gg}(\boldsymbol{\xi})$, a homogeneous non-Gaussian stochastic field $f(\mathbf{x})$ with power spectrum $S_{ff}^T(\boldsymbol{\kappa})$ can be defined as:

$$f(\mathbf{x}) = F^{-1} \cdot \Phi[g(\mathbf{x})] \quad (8)$$

where Φ is the standard Gaussian cumulative distribution function and F is the non-Gaussian marginal cumulative distribution function of $f(\mathbf{x})$. The transform $F^{-1} \cdot \Phi$ is a memory-less translation since the value of $f(\mathbf{x})$ at an arbitrary point $\mathbf{x} = (x, y)$ depends on the value of $g(\mathbf{x})$ at the same point only and the resulting non-Gaussian field is called a translation field (Grigoriu 1998).

Translation fields can be used to represent various non-Gaussian phenomena and have a number of useful properties such as the analytical calculation of crossing rates and extreme value distributions. They also have some limitations, the most important one from a practical point of view is that the choice of the marginal distribution of $f(\mathbf{x})$ imposes constraints to its correlation structure. In other words, F and $S_{ff}^T(\boldsymbol{\kappa})$, or $R_{ff}^T(\boldsymbol{\xi})$, have to satisfy a specific compatibility condition derived directly from the definition of the autocorrelation function of the translation field (Grigoriu 1998). If F and $S_{ff}^T(\boldsymbol{\kappa})$ are proven to be incompatible, there is no translation field with the prescribed characteristics. In this case, one has to resort to translation fields that match the target SDF approximately (Shields et al. 2011).

3.2 The Spectral Representation Method

In this paper, Eq. (8) is used for the generation of non-Gaussian translation sample functions representing the uncertain material properties of the problem. Sample functions of the underlying homogeneous Gaussian field $g(\mathbf{x})$ are generated using the spectral representation method (Shinozuka and Deodatis 1996). For a two-dimensional stochastic field, the i -th sample function is given by:

$$g^{(i)}(x, y) = \sqrt{2} \sum_{n_1=0}^{N_1-1} \sum_{n_2=0}^{N_2-1} [A_{n_1 n_2}^{(1)} \cos(\kappa_{1n_1} x + \kappa_{2n_2} y + \phi_{n_1 n_2}^{(1)(i)}) + A_{n_1 n_2}^{(2)} \cos(\kappa_{1n_1} x - \kappa_{2n_2} y + \phi_{n_1 n_2}^{(2)(i)})] \quad (9)$$

where $\phi_{n_1 n_2}^{(j)(i)}$, $j = 1, 2$ represent the realization for the i -th simulation of the independent random phase angles uniformly distributed in the range $[0, 2\pi]$. $A_{n_1 n_2}^{(1)}$, $A_{n_1 n_2}^{(2)}$ have the following expressions

$$A_{n_1 n_2}^{(1)} = \sqrt{2S_{gg}(\kappa_{1n_1}, \kappa_{2n_2})\Delta\kappa_1\Delta\kappa_2} \quad (10a)$$

$$A_{n_1 n_2}^{(2)} = \sqrt{2S_{gg}(\kappa_{1n_1}, -\kappa_{2n_2})\Delta\kappa_1\Delta\kappa_2} \quad (10b)$$

where

$$\kappa_{1n_1} = n_1 \Delta\kappa_1 \quad \kappa_{2n_2} = n_2 \Delta\kappa_2 \quad (11)$$

$$\Delta\kappa_1 = \frac{\kappa_{1u}}{N_1} \quad \Delta\kappa_2 = \frac{\kappa_{2u}}{N_2} \quad (12)$$

$$n_1 = 0, 1, \dots, N_1 - 1 \quad \text{and} \quad n_2 = 0, 1, \dots, N_2 - 1 \quad (13)$$

$N_j, j = 1, 2$, represent the number of intervals in which the wave number axes are subdivided and $\kappa_{ju}, j = 1, 2$, are the upper cut-off wave numbers which define the active region of the power spectrum $S_{gg}(\kappa_1, \kappa_2)$ of the stochastic field. The last means that S_{gg} is assumed to be zero outside the region defined by

$$-\kappa_{1u} \leq \kappa_1 \leq \kappa_{1u} \quad \text{and} \quad -\kappa_{2u} \leq \kappa_2 \leq \kappa_{2u} \quad (14)$$

The SDF used in the numerical example (see Sect. 5) is of square exponential type:

$$S_{gg}(\kappa_1, \kappa_2) = \sigma_g^2 \frac{b_1 b_2}{4\pi} \exp\left[-\frac{1}{4}(b_1^2 \kappa_1^2 + b_2^2 \kappa_2^2)\right] \quad (15)$$

where σ_g denotes the standard deviation of the stochastic field and b_1, b_2 denote the parameters that influence the shape of the spectrum, which are proportional to the correlation lengths of the stochastic field along the x, y axes, respectively. The squared exponential model is a realistic correlation model for softening materials (e.g. concrete) suggested by the Joint Committee on Structural Safety (JCSS 2001) and used in several publications, e.g. Vořechovský (2008), Yang and Xu (2008), and Eliáš et al. (2014). The SDF of the translation field will be slightly different from S_{gg} due to the spectral distortion caused by the transform of Eq. (8) (Papadopoulos et al. 2009).

4 Stochastic Finite Element Analysis

It is assumed that the Young's modulus E , tensile strength f_t and fracture energy G_f of the material are represented by two dimensional uni-variate (2D-1V) homogeneous stochastic fields. The variation of E is described as follows:

$$E(x, y) = E_0[1 + f(x, y)] \quad (16)$$

where E_0 is the mean value of the elastic modulus and $f(x, y)$ is a zero-mean homogeneous stochastic field. The two other properties are varying in a similar way. The stochastic stiffness matrix is derived using the midpoint method, i.e. one integration point at the centroid of each finite element is used for the computation of the stiffness matrix. This approach gives accurate results for relatively coarse meshes keeping the computational cost at reasonable levels (Stefanou 2009).

Using the procedure described in Sect. 3, a large number N_{SAMP} of sample functions are produced, leading to the generation of a set of stochastic stiffness

matrices. The associated structural problem is solved N_{SAMP} times and the response variability can finally be calculated by obtaining the response statistics of the N_{SAMP} simulations.

5 Numerical Example

The double-edge notched specimen under tension (Shi et al. 2000; Nguyen 2008) shown in Fig. 2 is used as a numerical example. The specimen is fixed in both directions at the bottom edge, and in horizontal direction at the top edge. Four-node linear quadrilateral elements under plane stress conditions and a 2×2 Gaussian integration rule are used in the numerical analyses. The uncertain parameters of the problem are the Young's modulus E , tensile strength f_t and fracture energy G_f of the material with mean values equal to 24 GPa, 2.4 MPa and 0.059 N/mm, respectively.

The spatial fluctuation of the uncertain parameters is described by 2D-1V homogeneous lognormal translation fields, sample functions of which are generated using Eqs. (8) and (9). A Weibull distribution could be adopted for the tensile strength f_t and fracture energy G_f , as in Vořechovský (2008) and Yang and Xu (2008), without leading to significant differences in the results. Three different values ($b = 1.2, 12, 120$) of the correlation length parameter b proportional to the dimensions of the structure are used, corresponding to stochastic fields of low, moderate and strong correlation (all values of b are in mm). Sample functions of

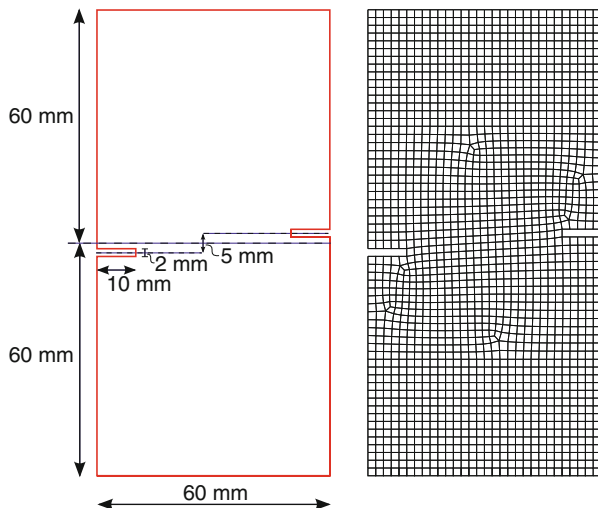


Fig. 2 Double-edge notched specimen (Geometry and FE mesh with 1,950 nodes and 1,850 elements)

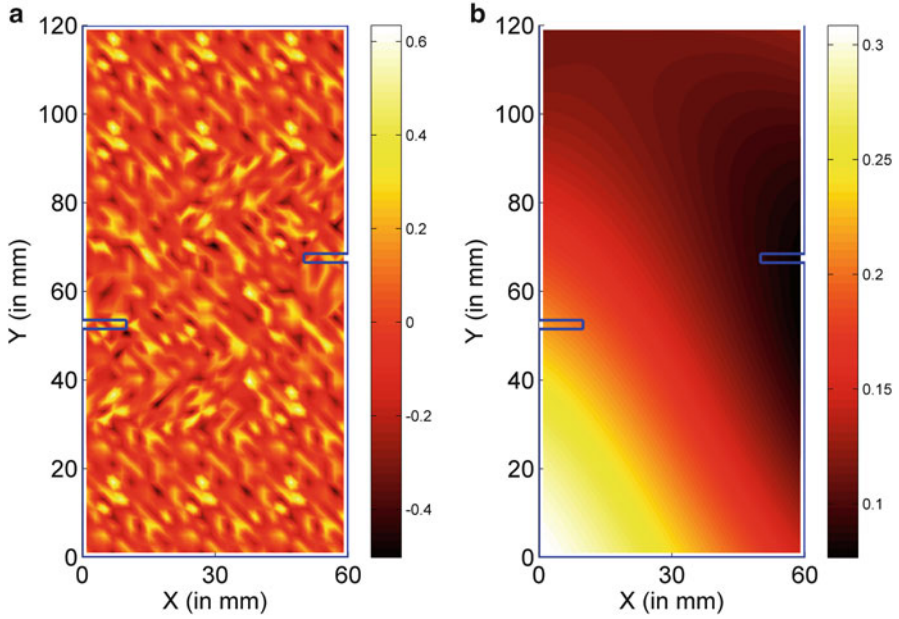


Fig. 3 Realizations of a lognormal field for $\sigma = 20\%$ and (a) $b = 1.2$, (b) $b = 120$

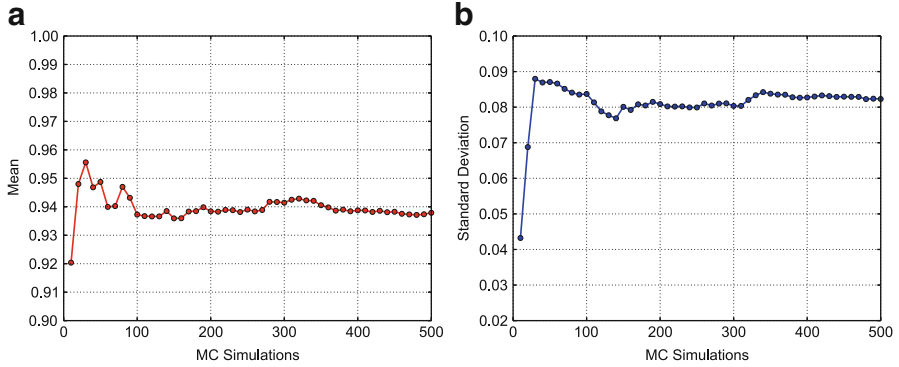


Fig. 4 Statistical convergence for (a) mean and (b) standard deviation of the peak load (E , f_t , G_f fully correlated with $\sigma = 10\%$ and $b = 120$)

a lognormal field for $\sigma = 20\%$ and $b = 1.2$, $b = 120$ are shown in Fig. 3a, b, respectively. The case of anisotropic correlation ($b_1 \neq b_2$) has also been examined to highlight its effect on the response variability, which is computed using direct MCS with a sample size equal to 500. The statistical convergence achieved within this number of samples is illustrated in Fig. 4 where the mean value and standard deviation of the peak load are plotted as a function of the number of simulations.

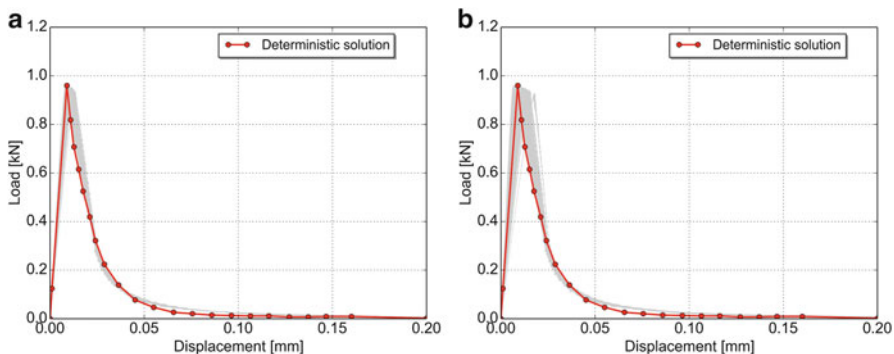


Fig. 5 Load-displacement curves for stochastic parameter E with (a) $\sigma = 10\%$ and (b) $\sigma = 20\%$ ($b = 120$)

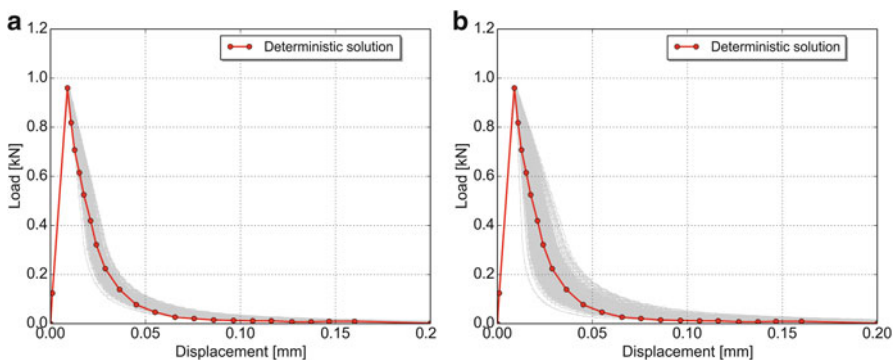


Fig. 6 Load-displacement curves for stochastic parameter G_f with (a) $\sigma = 10\%$ and (b) $\sigma = 20\%$ ($b = 120$)

Figures 5 and 6 show the load-displacement curves obtained from different stochastic simulations with variable E , G_f . Comparisons with the deterministic nonlinear solution of Nguyen (2008) are provided in these figures. As shown in Fig. 5, the variation of E affects the stiffness of the structure. The results obtained with the assumption of anisotropic correlation were very similar and therefore isotropic correlation ($b = b_1 = b_2$) is finally adopted. As a final step, two cases of combined variation of E , f_t , G_f are considered. In the first case, the lognormal stochastic fields representing the three parameters are fully correlated while in the second case there is no cross-correlation between them. The corresponding load-displacement curves shown in Fig. 7 are highly variable and thus lead to a large probability of failure p_f of the structure (defined as the probability of the peak load not exceeding that of the deterministic solution, which means that the structure fails at a smaller load). For $b = 1.2$, the peak load of all realizations is smaller than the deterministic one, while p_f is equal to 87 and 61 % for $b = 12$ and 120, respectively (case of fully correlated properties).

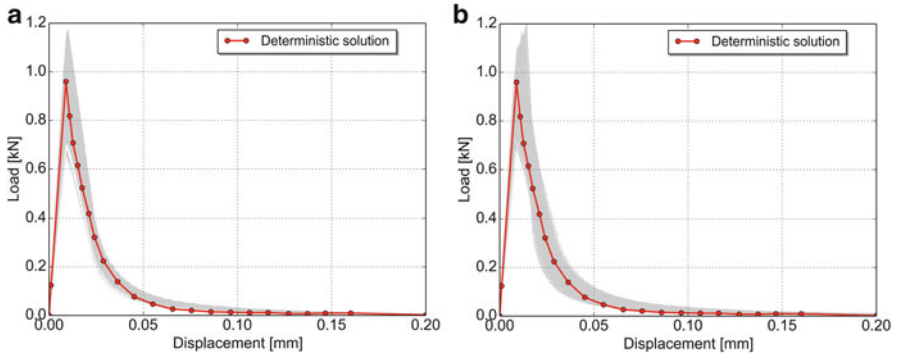


Fig. 7 Load-displacement curves for combined variation of the three parameters for $\sigma = 10\%$ ($b = 120$): (a) E, f_t, G_f fully correlated, (b) E, f_t, G_f uncorrelated

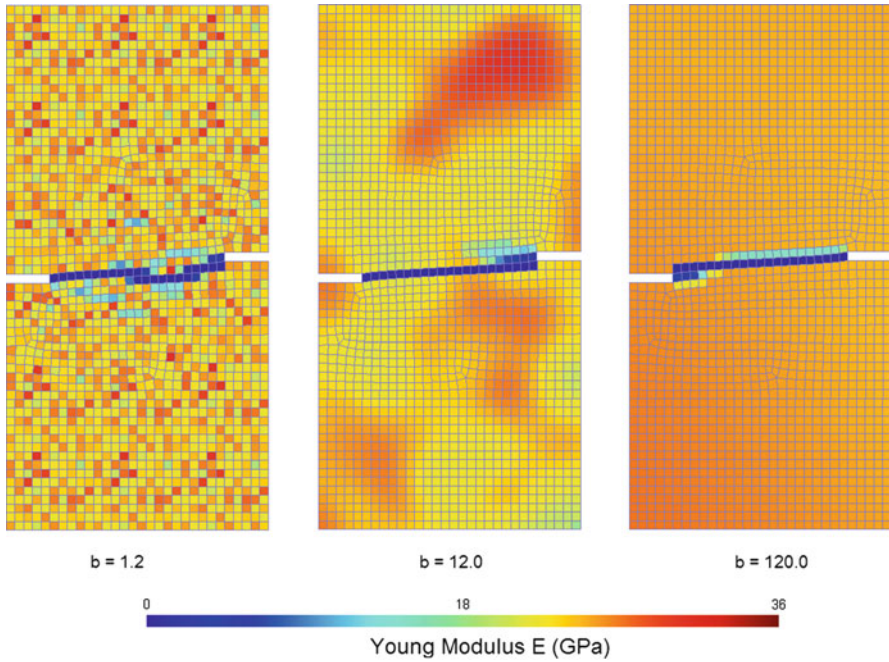


Fig. 8 Crack paths for a randomly selected realization and for different values of correlation length b (E, f_t, G_f fully correlated)

Finally, crack paths for a randomly selected realization and for different values of correlation length b are shown in Fig. 8 (the crack paths are formed by elements with zero stiffness at the end of SLA). The unrealistic crack pattern obtained for $b = 1.2$ is due to the high variability of the elastic modulus in this case which leads to neighboring elements with substantially different E .

6 Conclusions

In this work, the sequentially linear analysis is implemented in the framework of a stochastic setting to investigate the influence of uncertain spatially varying material properties on the fracture behavior of structures with softening materials. The proposed approach constitutes an efficient procedure avoiding the convergence problems encountered in regular nonlinear FE analysis. The uncertain properties are described by homogeneous stochastic fields using the spectral representation method in conjunction with translation field theory. The response variability is computed by means of direct MCS. The influence of the variation of each random parameter as well as of the coefficient of variation and correlation length of the stochastic fields has been quantified. The analysis of a benchmark structure has shown that the load-displacement curves, the crack paths and the probability of failure are affected by the statistical characteristics of the stochastic fields. The extension of SLA to the stochastic framework offers an efficient means to perform parametric investigations of the fracture behavior of structures with variable material properties. The possibility of using variability response functions as an alternative to MCS for computing the response variability of structures with softening materials in the framework of SLA is currently under investigation.

Acknowledgements This work is implemented within the framework of the research project “MICROLINK: Linking micromechanics-based properties with the stochastic finite element method: a challenge for multiscale modeling of heterogeneous materials and structures” – Action “Supporting Postdoctoral Researchers” of the Operational Program “Education and Lifelong Learning” (Action’s Beneficiary: General Secretariat for Research and Technology), and is co-financed by the European Social Fund (ESF) and the Greek State. The provided financial support is gratefully acknowledged. M. Papadrakakis acknowledges the support from the European Research Council Advanced Grant “MASTER-Mastering the computational challenges in numerical modeling and optimum design of CNT reinforced composites” (ERC-2011-ADG 20110209).

References

- Bazant ZP, Cedolin L (2010) Stability of structures: elastic, inelastic, fracture and damage theories. World Scientific, Hackensack
- De Borst R, Crisfield MA, Remmers JJC, Verhoosel CV (2012) Non-linear finite element analysis of solids and structures, 2nd edn. Wiley, Chichester
- DeJong MJ, Belletti B, Hendriks MA, Rots JG (2009) Shell elements for sequentially linear analysis: lateral failure of masonry structures. Eng Struct 31(7):1382–1392
- Eliáš J, Vořechovský M, Le JL (2014) Fracture simulations of concrete using discrete meso-level model with random fluctuations of material parameters. In: Proceedings of the IUTAM symposium on multiscale modeling and uncertainty quantification of materials and structures. Springer, Santorini Island, Greece
- Georgioudakis M, Stefanou G, Papadrakakis M (2014) Stochastic failure analysis of structures with softening materials. Eng Struct 61:13–21
- Grigoriu M (1998) Simulation of stationary non-Gaussian translation processes. J Eng Mech 124(2):121–126

- JCSS (2001) Probabilistic model code, part 3: resistance models. Joint Committee on Structural Safety. Published online at: <http://www.jcss.byg.dtu.dk/>
- Jirásek M (1998) Nonlocal models for damage and fracture: comparison of approaches. *Int J Solids Struct* 35(31–32):4133–4145
- Mariani S, Perego U (2003) Extended finite element method for quasi-brittle fracture. *Int J Numer Methods Eng* 58(1):103–126
- Moës N, Dolbow J, Belytschko T (1999) A finite element method for crack growth without remeshing. *Int J Numer Methods Eng* 46(1):131–150
- Nguyen GD (2008) A thermodynamic approach to non-local damage modelling of concrete. *Int J Solids Struct* 45(7–8):1918–1934
- Oliver J (1996) Modelling strong discontinuities in solid mechanics via strain softening constitutive equations. Part 1: fundamentals. *Int J Numer Methods Eng* 39(21):3575–3600
- Oliver J, Huespe A, Dias I (2012) Strain localization, strong discontinuities and material fracture: matches and mismatches. *Comput Methods Appl Mech Eng* 241–244:323–336
- Papadopoulos V, Stefanou G, Papadrakakis M (2009) Buckling analysis of imperfect shells with stochastic non-Gaussian material and thickness properties. *Int J Solids Struct* 46(14–15):2800–2808
- Rots J (2001) Sequentially linear continuum model for concrete fracture. In: de Borst R, Mazars J, Pijaudier-Cabot G, van Mier J (eds) *Fracture mechanics of concrete structures*. Balkema, Lisse, pp 831–839
- Rots JG, Invernizzi S (2004) Regularized sequentially linear saw-tooth softening model. *Int J Numer Anal Methods Geomech* 28(7–8):821–856
- Rots JG, Belletti B, Invernizzi S (2008) Robust modeling of RC structures with an “event-by-event” strategy. *Eng Fract Mech* 75(3–4):590–614
- Shi C, van Dam A, van Mier J, Sluys L (2000) Crack interaction in concrete. In: Wittmann F (ed) *Materials for buildings and structures. EUROMAT – vol 6*. Wiley, Weinheim, pp 125–131
- Shields M, Deodatis G, Bocchini P (2011) A simple and efficient methodology to approximate a general non-Gaussian stationary stochastic process by a translation process. *Probab Eng Mech* 26(4):511–519
- Shinozuka M, Deodatis G (1996) Simulation of multi-dimensional Gaussian stochastic fields by spectral representation. *Appl Mech Rev* 49(1):29–53
- Stefanou G (2009) The stochastic finite element method: past, present and future. *Comput Methods Appl Mech Eng* 198:1031–1051
- Vořechovský M (2008) Simulation of simply cross correlated random fields by series expansion methods. *Struct Saf* 30(4):337–363
- Yang Z, Xu XF (2008) A heterogeneous cohesive model for quasi-brittle materials considering spatially varying random fracture properties. *Comput Methods Appl Mech Eng* 197(45–48):4027–4039

Multiscale Modeling and Uncertainty Quantification of
Materials and Structures

Proceedings of the IUTAM Symposium held at Santorini,
Greece, September 9-11, 2013.

Papadrakakis, M.; Stefanou, G. (Eds.)

2014, IX, 306 p. 157 illus., 64 illus. in color., Hardcover

ISBN: 978-3-319-06330-0